Wave Profile Modification in Free-Electron Lasers: Space-Charge Transverse Fields and Optical Guiding

E. Jerby
Faculty of Engineering, Tel-Aviv University, Tel-Aviv, Israel

A. Gover[a]
Science Application International Corporation, McLean, Virginia 22101
(Received 23 August 1988)

A comparative analysis of wave profile modification effects in Raman free-electron lasers is presented. The analysis is based on a 3D theoretical model that is valid in both Raman and Compton regimes. We study two companion effects, the optical guiding and the excitation of space-charge waves with transverse field components. Both effects are compared through exemplary parameters based on previous free-electron laser experiments. We conclude that transverse field profile modification due to space-charge waves may be significant in comparison to the optical guiding effect.

PACS numbers: 42.55.Tb

Modification of the radiation wave profile, due to the free-electron laser (FEL) interaction, is a subject of significant interest in recent FEL research. It was predicted that at high gain levels an effect of *optical guiding* of the electromagnetic wave by the e beam may take place.[1,2] This effect enables a high optical filling factor, and consequently high gain, even with wigglers much longer than the Rayleigh length of the optical beam. Thus, some of the very-high-intensity long wiggler FEL experiments, presently under development, rely on the existence of the optical guiding effect. However, wave profile modification in FEL's may be a consequence of other effects, besides the optical guiding effect. A primary companion effect is the excitation of Langmuir space-charge waves, which in a 3D model may have, as we subsequently show, a nonnegligible transverse field amplitude.

Experimental measurements of wave profile modification in Raman FEL's were recently reported.[3,4] Rigorous analysis of the experimental results requires a clear distinction between the optical guiding and the excitation of space-charge waves with transverse fields. In previous theoretical works the optical guiding[1,2,5] and some 3D features of the space-charge waves in FEL[5-7] were analyzed separately. In this paper we analyze distinctively these two effects by using a general semianalytical technique to solve the linear 3D FEL problem.

The 3D model[8,9] is based on the expansion of the Maxwell and Boltzman equations by Fourier decomposition in the t,x,y dimensions, and Laplace transform in the propagation dimension, z. This leads in general to a matrix gain-dispersion relation (GDR), which is solved numerically. The 3D model is applicable to an arbitrary electron-beam distribution in free space or in a waveguide. Using the perturbation method, the Maxwell and Vlasov equations result in a set of coupled linear differential equations for the field $\mathbf{E}(\mathbf{x},\omega)$ and the perturbation to the electron distribution function $f_1(\mathbf{p},\mathbf{x},\omega)$

$$\nabla^2\mathbf{E}(\mathbf{x},\omega)+k_0^2\mathbf{E}=e\mu_0 i\omega\int_{\mathbf{p}}\mathbf{v}f_1 d^3p-\frac{e}{\epsilon_0}\nabla\int_{\mathbf{p}}f_1 d^3p\,, \quad (1)$$

$$\mathbf{v}\cdot\nabla f_1(\mathbf{p},\mathbf{x},\omega)+\mathbf{F}_0\cdot\nabla_{\mathbf{p}}f_1=i\omega f_1-\mathbf{F}_1\cdot\nabla\mathbf{p}f_0\,. \quad (2)$$

The time-independent periodic force, $\mathbf{F}_0=-e\mathbf{v}\times\mathbf{B}_W$, imposed by the static wiggler field, $\mathbf{B}_W=\mathrm{Re}\{\mathbf{B}_{W0}e^{-ik_W z}\}$, is assumed to be much stronger than the time-dependent first-order Lorentz force, $\mathbf{F}_1(\mathbf{p},\mathbf{x},\omega)=-e(\mathbf{E}+\mathbf{v}\times\mu_0\mathbf{H})$, that is exerted by the time-dependent electrostatic (space-charge) and electromagnetic fields (**E**, **H**). Equation (2) is a linear, partial differential equation of first order; thus the method of characteristic lines is applied to solve it. Its characteristic lines are identical to those of the zero-order Vlasov equation, $\mathbf{v}\cdot\nabla f_0(\mathbf{p},\mathbf{x})+\mathbf{F}_0\cdot\nabla_{\mathbf{p}}f_0=0$, and are given by the solutions of the unperturbed equation of electron motion $(\mathbf{V}_{\mathrm{ch}}\cdot\nabla)\mathbf{p}_{\mathrm{ch}}=\mathbf{F}_0$.

The equation set is transformed to the spatial frequency domain, using the transverse spatial Fourier transform,

$$\bar{E}(\mathbf{k}_\perp)=\int_{\mathbf{x}_\perp}E(\mathbf{x}_\perp)\exp(i\mathbf{k}_\perp\cdot\mathbf{x}_\perp)d\mathbf{x}_\perp\,.$$

In a Cartesian coordinate system and finite transverse dimensions, the transverse wave-number vector is discretized according to $\mathbf{k}_\perp=\hat{\mathbf{x}}mk_{x0}+\hat{\mathbf{y}}nk_{y0}$, where $m,n=0,\pm1,\pm2,\ldots$. For rectangular waveguide FEL schemes,[3,10] $k_{x0}=\pi/a$, $k_{y0}=\pi/b$, where a and b are the corresponding x and y dimensions of the waveguide. Equation (2) is integrated along the characteristic $\mathbf{V}_{\mathrm{ch}}(\mathbf{p}_0,\mathbf{x}_0,z)$, and the first-order distribution function, expressed in the spatial frequency domain is found to be

$$\bar{f}_{1c}(\mathbf{p}_0,\mathbf{k}_\perp,z)=-e^{-i\phi_c(z)}\int_{z'=0}^{z}\bar{F}_{1c}*\cdot\nabla_{\mathbf{p}}\bar{f}_{0c}(\mathbf{p}_0,\mathbf{k}_\perp,z=0)e^{i\phi_c(z')}dz'/V_{c0z}(z')\,, \quad (3)$$

where the phase term is given by

$$\phi_c(z)=\int_{z'=0}^{z}(\mathbf{V}_{c0\perp}\cdot\mathbf{k}_\perp-\omega)dz'/V_{c0z}(z')\,.$$

The asterisk symbol, $*$, denotes a convolution operation in the spatial frequencies domain, $\mathbf{k}_\perp$. Applying now Laplace integral transform,

$$\tilde{f}(s)\equiv\mathcal{L}\{f(z)\}\equiv\int_{z=0}^{\infty}f(z)\exp(-sz)dz\,,$$

the original set [Eqs. (1) and (2)] reduces into an algebraic set:

$$(s^2+k_0^2-|\mathbf{k}_\perp|^2)\tilde{\bar{\mathbf{E}}}(s,\mathbf{k}_\perp,\omega)-s\bar{E}_0-\bar{E}_0'=\frac{e}{\epsilon_0}\int_{\mathbf{p}_0}\left\{\frac{i\omega}{c^2}[\mathbf{V}_W\tilde{\bar{f}}_1(s+ik_W)+\mathbf{V}_W^*\tilde{\bar{f}}_1(s-ik_W)]+\left[\left(\frac{i\omega}{c^2}\bar{v}_z-s\right)\hat{\mathbf{z}}-i\mathbf{k}_\perp\right]\tilde{\bar{f}}_1(s)\right\}d^3p\,,\tag{4}$$

$$\tilde{\bar{f}}_1(s,\mathbf{k}_\perp,\omega)\cong\frac{-1}{s-i\omega/\bar{v}_z}\tilde{\bar{F}}(s)*\cdot\nabla_{\mathbf{p}}\bar{f}_{0c}/\bar{v}_z\,,\tag{5}$$

where the characteristic line, on axis, is $\mathbf{V}_{c0}=\mathrm{Re}\{\mathbf{V}_W e^{-ik_W z}\}+\hat{\mathbf{z}}\bar{v}_z$ and

$$\tilde{\bar{F}}(s,\mathbf{k}_\perp,\omega)=-e\{\tilde{\bar{E}}(s)+\tfrac{1}{2}\mu_0[\mathbf{V}_W\times\tilde{\bar{H}}(s+ik_W)+\mathbf{V}_W^*\times\tilde{\bar{H}}(s-ik_W)]\}\,.$$

For a planar wiggler $\mathbf{V}_W=\hat{\mathbf{x}}eB_W/\gamma mk_W$. The zero-order distribution function is taken to be $f_0(\mathbf{p}_0,\mathbf{x}_\perp)=n_0f_{p_z}(p_z)\times g_0(\mathbf{x}_\perp)$, assuming that the initial momentum spread is independent of $\mathbf{x}_\perp$, and that the transverse profile $g_0(\mathbf{x}_\perp)$ is conserved along the interaction region. Equations (4) and (5) become an infinite set for $-\infty<l,m,n<\infty$,

$$[(s+ilk_W)^2+k_0^2-m^2k_{0x}^2-n^2k_{0y}^2]\tilde{\bar{\mathbf{E}}}^{(l)}_{\perp m,n}-(s+ilk_W)\bar{E}_{0\perp m,n}-\bar{E}'_{0\perp m,n}=\hat{\mathbf{x}}\frac{\omega^2V_{Wx}}{2ec^2\langle\bar{v}_z\rangle}\bar{g}_0*[\tilde{\bar{\mathbf{F}}}^{(l-1)}\cdot\boldsymbol{\chi}_{\mathbf{p}}^{(l-1)}+\tilde{\bar{\mathbf{F}}}^{(l+1)}\cdot\boldsymbol{\chi}_{\mathbf{p}}^{(l+1)}]-\frac{\omega}{e\langle\bar{v}_z\rangle}(\hat{\mathbf{x}}mk_{0x}+\hat{\mathbf{y}}nk_{0y})\bar{g}_0*\tilde{\bar{\mathbf{F}}}^{(l)}\cdot\boldsymbol{\chi}_{\mathbf{p}}^{(l)}\,,\tag{6}$$

$$[(s+ilk_W)^2+k_0^2-m^2k_{0x}^2-n^2k_{0y}^2]\tilde{\bar{E}}^{(l)}_{z_{m,n}}=-\frac{\omega^2}{e\gamma_z^2\langle\bar{v}_z\rangle^2}\bar{g}_0*\tilde{\bar{\mathbf{F}}}^{(l)}\cdot\boldsymbol{\chi}_{\mathbf{p}}^{(l)}\,,\tag{7}$$

where $E^{(l)}(\mathbf{k}_\perp,s)\equiv E(\mathbf{k}_\perp,s+lik_W)$, $l=0,\pm1,\pm2,\ldots$, and the e-beam susceptibility function,[11] shifted in the s plane by ilk_W, $\chi_{\mathbf{p}}^{(l)}\equiv\chi_{\mathbf{p}}(\omega,s+ilk_W)$, is defined as

$$\chi_{\mathbf{p}}^{(l)}\equiv\frac{e^2n_0}{i\epsilon_0\omega}\int_{\mathbf{p}_0}\frac{\nabla_{\mathbf{p}}f_{\mathbf{p}}(\mathbf{p}_0)}{s+ilk_W-i\omega/\bar{v}_z}d^3p_0\,.\tag{8}$$

Equations (6) and (7) are an *s-plane* representation of the Floquet theorem for periodic structures, and the unknowns of the algebraic equation $E^{(l)}(\mathbf{k}_\perp,s)$ are the transformed space harmonics of the FEL interaction Floquet modes. Equation (6) contains three susceptibility terms, $\chi_{\mathbf{p}}^{(l\pm1)}$ and $\chi_{\mathbf{p}}^{(l)}$, that according to Eq. (8) have singularities at $s+(l\pm1)ik_W-i\omega/\bar{v}_z=0$ and $s+lik_W-i\omega/\bar{v}_z=0$, respectively. However, assuming that the system operates in the vicinity of the uncoupled electromagnetic (EM) wave poles (i.e., $s\sim s_0=ik_{0z}$), the singularity that may have the most considerable effect on $\mathbf{E}_\perp^{(0)}$ is $s_0+ik_W-i\omega/\bar{v}_z\sim0$, which is attained near the synchronism condition $\omega/(k_{0z}+k_W)\sim\bar{v}_z$. Therefore, $\chi_{\mathbf{p}}^{(l+1)}\gg\chi_{\mathbf{p}}^{(l\neq1)}$, and out of the infinite set of Eqs. (6) and (7), $-\infty<l<\infty$, one may keep only the equations for $l=0,1,2$. The zero-order space harmonic ($\mathbf{E}_\perp^{(0)}\equiv\mathbf{E}^{\mathrm{EM}}$) is composed predominantly of a solenoidal field, namely EM radiation modes of the waveguide. Its wave-number spectrum is nearly matched to the wave number of the input radiation mode $s/i\sim k_{0z}$ and it propagates at a phase velocity that is nearly $\omega/k_{0z}\geq c$. On the other hand, the first-order harmonic ($\mathbf{E}^{(+1)}\equiv E^{\mathrm{ES}}$) is composed predominantly of irrotational fields,[12] namely electrostatic (ES) modes of the e-beam plasma. Its wave-number spectrum $s/i+k_W\sim k_{0z}+k_W$ is matched to the wave numbers of the space-charge waves of the beam and its phase velocity is approximately the speed of the e beam and the space-charge waves, $\omega/(k_{0z}+k_W)\sim\bar{v}_{0z}$. The second-order space harmonic $\mathbf{E}^{(+2)}$ is smaller than $\mathbf{E}^{(+1)}$ and its negligibility was confirmed by numerical calculation. The different plane-wave (angular spectrum) coefficients ($-\infty<m,n<\infty$) are coupled to each other through the discrete convolution $*$ on the right-hand side of Eqs. (6) and (7).

The FEL equation set [(6) and (7)] is rewritten in a compact matrix form as follows:

$$\underline{K}^{(0)}\cdot\underline{E}_X^{(0)}-\underline{\hat{E}}_{X0}=\frac{\omega^2V_{Wx}}{4ec^2\langle\bar{v}_z\rangle s}\underline{G}\cdot\underline{F}_Z^{(+1)}\chi_z^{(+1)}\,,\tag{9a}$$

$$\underline{F}_Z^{(+1)}=-e\underline{E}_Z^{(+1)}-\frac{e}{2i\omega}V_{Wx}s\underline{E}_X^{(0)}\,,\tag{9b}$$

$$\underline{K}^{(+1)}\cdot\underline{E}_Z^{(+1)}=\frac{\omega^2}{2e\langle\gamma_z^2\bar{v}_z^2\rangle(s+ik_W)}\underline{G}\cdot\underline{F}_Z^{(+1)}\chi_z^{(+1)}\,,\tag{9c}$$

$$\underline{K}^{(+1)}\cdot\underline{E}_X^{(+1)}=-\frac{\omega}{2e\langle\bar{v}_z\rangle s}(\hat{\mathbf{x}}k_{0x}\underline{M}+\hat{\mathbf{y}}k_{0y}\underline{N})\times\underline{GF}_Z^{(+1)}\chi_z^{(+1)}\,.\tag{9d}$$

The elements of the transverse electric field vector are the spatial frequency spectral components of the transverse electric field, $\underline{E}_X = \{\hat{\mathbf{E}}_{x_{m,n}}(s)\}$ and $\underline{\hat{E}}_{X0} = \{\bar{E}_{x0_{m,n}}(z=0)\}$. The components of the ponderomotive force vector $\underline{F}_Z$ and the other vectors are similarly defined. The vectors are truncated in the angular spectrum space to the number of plane waves required for proper description of the 3D features of the problem.[8,9] The longitudinal component, $\chi_z^{(+1)} = \hat{\mathbf{z}} \cdot \boldsymbol{\chi}_{\mathbf{p}}^{(+1)}$, is the dominant term of the susceptibility integral (8). The 3D profile matrix $\underline{G}$ is the matrix representation for the convolution operation in the $\mathbf{k}_\perp$ space. It is composed of the Fourier components of the e-beam profile $\bar{g}_{m,n}$. The diagonal matrices $\underline{M}$ and $\underline{N}$ are composed of elements $m_{ii} = m$, $n_{ii} = n$, which are the mode index numbers. The diagonal matrix $\underline{K}^{(l)}$ is composed of elements

$$k_{ii}^{(l)} = [(s + ilk_W)^2 + k_0^2 - n^2 k_{0x}^2 - m^2 k_{0y}^2]/2(s + ilk_W) .$$

The EM ($l=0$) and ES ($l=1$) matrix GDR's are derived now from the matrix equations (9a)–(9d). The matrix GDR for the EM waves is

$$\underline{E}_X^{(0)}(s) = \{[\underline{I} + \underline{R}\chi_z^{(+1)}]\underline{K}^{(0)} - i\kappa\underline{G}\chi_z^{(+1)}\}^{-1}[\underline{I} + \underline{R}\chi_z^{(+1)}]\underline{\hat{E}}_{X0}(z=0) , \tag{10}$$

and the corresponding equations for the ES waves are

$$\underline{E}_Z^{(+1)}(s) = \frac{isV_{Wx}}{2\omega}\underline{R}'\chi_z^{(+1)}\{\underline{K}^{(0)}[\underline{I} + \underline{R}'\chi_z^{(+1)}] - i\kappa\underline{G}\chi_z^{(+1)}\}^{-1}\underline{\hat{E}}_{X0}(z=0) , \tag{11}$$

$$\underline{E}_\perp^{(+1)}(s) = \frac{\gamma_z^2\langle\bar{v}_z\rangle}{\omega}(\hat{\mathbf{x}}k_{0x}\underline{M} + \hat{\mathbf{y}}k_{0y}\underline{N})\underline{E}_Z^{(+1)}(s) . \tag{12}$$

The space-charge reduction matrices are defined as

$$\underline{R} = -\omega^2[2\langle\gamma_z^2\bar{v}_z^2\rangle(s + ik_W)]^{-1}\underline{G}\underline{K}^{(+1)^{-1}} ,$$

$$\underline{R}' = -\omega^2[2\langle\gamma_z^2\bar{v}_z^2\rangle(s + ik_W)]^{-1}\underline{K}^{(+1)^{-1}}\underline{G} .$$

The matrix $\underline{I}$ is a unit matrix. The coupling parameter

$$\kappa = \omega V_{Wx}^2/8c^2\langle\bar{v}_z\rangle = \tfrac{1}{8}k_0 a_W^2/\beta_z\gamma^2$$

is the same as in the 1D GDR.[13] The evolution of the fields in space can now be produced by substituting Eqs. (10)–(12) in the expansion

$$E(x,y,z) = \mathcal{L}^{-1}\left\{\sum_{\mathbf{k}_\perp} E(\mathbf{k}_\perp, s)e^{i\mathbf{k}_\perp \cdot \mathbf{x}_\perp}\right\} ,$$

and performing the inverse Fourier and Laplace transforms.

The significance of the various matrix terms in the GDR's [Eqs. (10)–(12)] becomes clearer when one examines them in the limit of a single mode (1D model).[13] In this case $\underline{I} + \underline{R}\chi_z^{(+1)} \to 1 + r\chi_a^{(+1)}$ is the longitudinal plasma permitivity, where r is the finite cross-section plasma reduction factor,[7] $\underline{K}^{(0)} \to s - ik_{0z}$ is the wave-number modification due to FEL interaction, $\underline{G}$ reduces to the optical filling factors A_e/A_{em}, and the EM GDR (10) reduces to the 1D scalar GDR.[13] The vector solutions of the matrix plasma permitivity $(\underline{I} + \underline{R}'\chi_z^{(+1)})\underline{E}_Z^{(+1)} = 0$ are the plane-wave expansion coefficients of the beam plasma eigenmodes.[7] The eigenvectors of the matrix in (10) are the expansion coefficients of the optical guided modes.[2,5]

In order to study the EM and ES wave profile modification effects and their relative importance, we employed the 3D FEL formulation on two examples, based on the data of the MIT[3] and LLNL[10] experiments. Both experiments used rectangular waveguides. The input waves in both cases are defined as the TE_{01} mode, composed of plane waves $m = 0$, $n = \pm 1$ (this is the fundamental mode in the MIT case). For the sake of simplicity and comparison, the wiggler polarization was taken as linear in the y direction in both cases. The results of the numerical computation are displayed comparatively in Fig. 1. Comparison of the EM wave solutions [Figs. 1(a)–1(d)] indicates evolution of optical guiding with the LLNL parameters (the LLNL results are shown for $z = 1$ m, for which operation is still in the linear regime). On the other hand, no significant modification to the EM wave profile (the $\mathbf{E}_\perp^{(0)}$ space harmonic) is observed with the MIT parameters and we must conclude that optical guiding is negligible in this case. The inclusion of evanescent x-polarized higher-order waveguide modes, in our formulations, did not help to produce optical guiding in the latter case. These are reasonable results, taking into account that in the MIT example the next modes (the TE_{02} and the TE_{10}) are decaying at a rate of 248 m^{-1}, whereas the LLNL experiment employs an overmoded waveguide. The Columbia FEL parameters,[4] modified to a rectangular waveguide, yields results similar to the LLNL case.

Examination of the ES wave profile curves [Figs. 1(e)–1(h)] indicates that in both examples substantial space-charge fields are built up and that the transverse field components are not negligible, and are even greater than the axial components. The transverse electrostatic field components, $\mathrm{Re}\{E_x^{ES}(x,y)\}$ and $\mathrm{Re}\{E_y^{ES}(x,y)\}$, are essentially the fringe fields of the beam space-charge bunches and therefore are antisymmetric and vanish on the axis. The longitudinal field $E_z^{ES}(x,y)$ is symmetric.

When interpreting experimental results of transverse

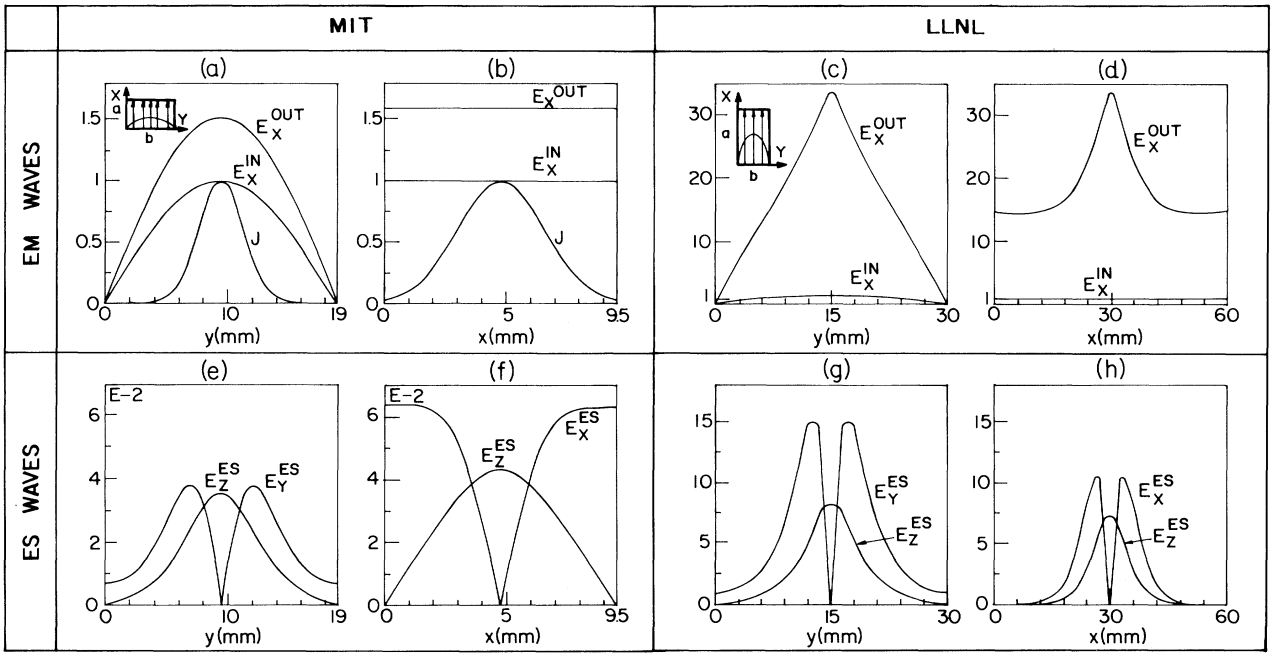

FIG. 1. A comparison of the electromagnetic and the electrostatic wave profiles (absolute values), calculated for examples based on the MIT [$I=\int J(x,y)dx\,dy=1$ A, $\gamma=1.39$, $A_e=\pi 2.5^2$ mm^2, $B_W=250$ G, $\lambda_W=3.3$ cm, $\lambda=2.8$ cm, $L_W=1.32$ m] and the LLNL ($I=850$ A, $\gamma=6.9$, $A_e=6\times 3$ mm^2, $B_W=3.7$ kG, $\lambda_W=9.8$ cm, $\lambda=8.6$ mm, $L_W=1$ m) FEL experiments.

probe measurements of the field profiles inside the waveguide,[3] one must be aware that the power $P(x,y)$ measured by the probe is relative to $|E_x^{EM}+E_x^{ES}|^2$. The probes measure the intensity in both equal frequency fields $|E_x^{EM}|^2$ and $|E_x^{ES}|^2$, but also measure their interference term $2\mathrm{Re}\{E_x^{EM}E_x^{ES*}\}$. Even when $|E_x^{ES}| \ll |E_x^{EM}|$, this interference term can produce a significant contribution. For the MIT parameters example this term can produce a transverse profile measurement variation of more than 10%, while for the LLNL parameters the measurable variation may exceed 60%.

The conclusion of our analysis and computation is that, contrary to a common assumption, the transverse field components of the excited space-charge waves can produce a significant modification to the measured transverse field profile in the parameter regime of Raman FEL's. While our model predicts optical guiding (in the sense of concentrating the profile of the fundamental EM space harmonic) in the LLNL case,[10] a similar effect (in the same limited sense) is not predicted with the parameters of the MIT experiment.[3] Some new measurements in the MIT experiment[14] tend to support our prediction and interpretation.

We acknowledge communications with G. Bekefi, J. Wurtele, and A. Fruchtman. This work was supported in part by the U.S. ONR Contract No. N00014-87-C0362.

[a]On leave from Tel Aviv University, Tel-Aviv, Israel.

[1]E. T. Scharlemann, A. M. Sessler, and J. M. Wurtele, Phys. Rev. Lett. **54**, 1925 (1985).

[2]G. T. Moore, Nucl. Instrum. Methods Phys. Res., Sect. A **239**, 19 (1985).

[3]F. Hartemann, K. Xu, G. Bekefi, J. S. Wurtele, and J. Fajans, Phys. Rev. Lett. **59**, 1177 (1987).

[4]A. Bhattacharjee, S. Y. Cai, S. P. Chang, J. W. Dodd, and T. C. Marshall, Phys. Rev. Lett. **60**, 1254 (1988).

[5]A. Fruchtman, Phys. Rev. A **37**, 2989 (1988).

[6]H. P. Freund and A. K. Ganguly, Phys. Rev. A **28**, 3438 (1983).

[7]B. Steinberg, A. Gover, and S. Ruschin, Phys. Rev. A **36**, 147 (1987).

[8]E. Jerby, Ph.D. dissertation, Tel Aviv University, 1988 (unpublished).

[9]E. Jerby and A. Gover, Nucl. Instrum. Methods Phys. Res., Sect. A **272**, 380 (1988).

[10]T. J. Orzechowski, E. T. Scharlemann, and B. D. Hopkins, Phys. Rev. A **35**, 2184 (1987).

[11]E. Jerby, Nucl. Instrum. Methods Phys. Res., Sect. A **272**, 457 (1988).

[12]M. Kisliuk, Int. J. Electronics **54**, 349 (1983).

[13]E. Jerby and A. Gover, IEEE J. Quantum Electron. **21**, 1041 (1985).

[14]K. Xu, G. Bekefi, and C. Leibovitch (to be published).